npj | parkinson's disease

Article

Published in partnership with the Parkinson's Foundation

https://doi.org/10.1038/s41531-024-00855-3

Systemically circulating 17β-estradiol enhances the neuroprotective effect of the smoking cessation drug cytisine in female parkinsonian mice

Sara M. Zarate[1,3], Roger C. Garcia[1,3], Gauri Pandey[1,2,3] & Rahul Srinivasan[1,2]

The smoking cessation drug cytisine exerts neuroprotection in substantia nigra pars compacta (SNc) dopaminergic (DA) neurons of female but not male 6-hydroxydopamine (6-OHDA) lesioned parkinsonian mice. To address the important question of whether circulating 17β−estradiol mediates this effect, we employ two mouse models aimed at depleting systemically circulating 17β-estradiol: (**i**) bilateral ovariectomy (OVX), and (**ii**) aromatase inhibition with systemically administered letrozole. In both models, depleting systemically circulating 17β-estradiol in female 6-OHDA lesioned parkinsonian mice results in the loss of cytisine-mediated neuroprotection as measured using apomorphine-induced contralateral rotations and SNc DA neurodegeneration. Our experiments also reveal that OVX alone exerts neuroprotection in SNc DA neurons due to compensatory changes not observed in the letrozole model, which underscores the importance of using independent models of 17β-estradiol depletion to study neuroprotection. Taken together, our findings suggest that the smoking cessation drug cytisine is a viable neuroprotective drug for pre-menopausal women with Parkinson's disease.

Epidemiological studies over the past 60 years demonstrate that smokers and chronic tobacco users are at a 50% reduced risk for Parkinson's disease (PD)[1–4]. In this context, we and others have shown that at smoking relevant nanomolar concentrations, nicotine, which is the major addictive ingredient of tobacco, binds to and stabilizes the high sensitivity $(\alpha4)_2(\beta2)_3$ stoichiometry of neuronal nicotinic acetylcholine receptors (nAChRs) within the endoplasmic reticulum (ER) of cells[5–9]. In subsequent studies, we showed that nicotine chaperones nAChRs out of the ER via Sec24D-containing ER exit sites (ERES) into the cellular secretory pathway[10–12]. Importantly, nicotine-mediated nAChR chaperoning in dopaminergic (DA) neurons is associated with an upregulation of Sec24D-containing ERES and an inhibition of all three signaling arms of the ER stress response pathway[12]. Given the established role of hyperactive ER stress in causing DA neuron loss during PD[13,14], our studies point to the general concept that nicotinic ligands can inhibit pathological ER stress signaling via nAChR chaperoning and ER exit site upregulation in DA neurons. Although this mechanism likely contributes to the neuroprotective effect of chronic tobacco use against PD, clinical trials employing nicotine as a disease-modifying treatment strategy for PD have failed, partly because of the adverse autonomic effects associated with large doses of systemic nicotine[15–19].

The smoking cessation drug cytisine is a partial agonist for α4β2 nAChRs with minimal side effects in humans[20]. In addition, cytisine can bind to and chaperone α4β2 nAChRs at low nanomolar concentrations[7,11,21]. Based on these favorable pharmacodynamic properties, we hypothesized that low nanomolar concentrations of cytisine could mediate neuroprotective effects against PD via the upregulation of nAChRs and ER exit sites and a consequent inhibition of the ER stress response in substantia nigra pars compacta (SNc) DA neurons. We tested this hypothesis in vivo by employing a preclinical mouse model of parkinsonism with unilateral injection of 6-hydroxydopamine (6-OHDA) into the dorsolateral striatum (DLS). Surprisingly, we found that when compared to saline-treated controls, systemically administered low-dose cytisine reduced the loss of SNc DA neurons only in female and not in male mice exposed to 6-OHDA[21]. Using mouse midbrain neuron-astrocyte co-cultures, we found that cytisine inhibited two arms of ER stress signaling: Activating transcription factor 6 (ATF6) and X-box binding protein 1 (XBP1). Furthermore, the active

[1]Department of Neuroscience & Experimental Therapeutics, Texas A&M University College of Medicine, 8447 John Sharp Pkwy, Bryan, TX, 77807-3260, USA. [2]Texas A&M Institute for Neuroscience (TAMIN), Interdisciplinary Life Sciences Building (ILSB), 3474 TAMU, College Station, TX, 77843-3474, USA. [3]These authors contributed equally: Sara M. Zarate, Roger C. Garcia, Gauri Pandey. e-mail: rahul@tamu.edu

metabolite of estrogen, 17β-estradiol, inhibited the expression of C/EBP homologous protein (CHOP), which is a downstream apoptotic mediator of the third arm of ER stress signaling[21]. Taken together, these findings suggest that 17β-estradiol acts in combination with cytisine to inhibit all three arms of the ER stress response (ATF6, XBP1 and CHOP), thereby exerting sex-specific neuroprotection in female parkinsonian mice.

A major question that arises from our finding that cytisine exerts neuroprotection only in female parkinsonian mice is whether systemically circulating 17β-estradiol is essential for cytisine to exert neuroprotection of SNc DA neurons in vivo. This is a particularly important question because understanding the role of 17β-estradiol in cytisine-mediated neuroprotection could enable future use of cytisine as a neuroprotective treatment for both men and women with PD. Based on this rationale, the present study examines the extent to which systemically circulating 17β-estradiol is necessary for cytisine-mediated neuroprotection in a 6-OHDA-induced preclinical mouse model of parkinsonism. We employ two types of manipulations to deplete systemically circulating 17β-estradiol in female mice, *viz.* bilateral ovariectomy (OVX) and pharmacological inhibition of aromatase (AROM) with the AROM inhibitor, letrozole. In each of the two models with depleted systemically circulating 17β-estradiol, we show that cytisine fails to exert neuroprotection in female 6-OHDA-exposed parkinsonian mice. Additionally, we demonstrate that treatment of OVX 6-OHDA mice with a combination of exogenous 17β−estradiol and cytisine rescues this neuroprotective effect. Thus, our results suggest that systemically circulating 17β-estradiol is indeed essential for cytisine to exert neuroprotection in a unilateral 6-OHDA mouse model of parkinsonism. Our study has important implications for developing combined formulations of cytisine and estrogen analogs as a clinically translatable neuroprotective treatment for men and women with PD. Furthermore, this study underscores the importance of using multiple independent methods to assess the effects of circulating 17β-estradiol on neuroprotection in rodent models of parkinsonism.

Methods

Mice

Two- to three-month-old female C57Bl6 mice were maintained on a 12-hour light-dark cycle. Food and water were provided *ad libitum*. All animal experiments were approved by the Texas A&M University Institutional Animal Care and Use Committee (IACUC Animal Use Protocol #2022-0252). Mice allocation to each experimental group was randomized before starting experiments. Sample sizes were determined based on previously published studies measuring the effect of cytisine on parkinsonian behaviors and SNc DA neuron loss[21]. To minimize potential confounders, each cage consisted of mice belonging to different treatment groups within a single experiment. All experiments in this study are reported in accordance with the ARRIVE guidelines.

Bilateral ovariectomy (OVX)

Mice were induced with 5% isoflurane and maintained with 2-3% isoflurane throughout the procedure. Fur was removed 2-3 cm lateral to the midline using clippers and the area was sterilized with 3 applications of iodine followed by 70% ethanol. Two 1-2 cm long incisions parallel to the midline were made through the skin and underlying muscle to access the ovaries. The uterine horns just proximal to the ovaries were tied off using polyglycolic acid-absorbable synthetic sutures. The ovaries and surrounding fat were then excised. For sham surgeries, the ovaries were accessed but not removed. Post-operative monitoring was performed for one week after OVX to ensure proper wound healing. Only mice that showed no signs of pain or distress for one week following OVX were used in experiments.

Unilateral lesion of the dorsolateral striatum (DLS) with 6-OHDA

All mice were anesthetized with isoflurane as described for OVX, and unilateral stereotaxic injection of 10 µg 6-OHDA in the dorsolateral striatum (DLS) was performed as previously described[21]. Briefly, 2 µl of a 5 mg/ml stock solution of 6-OHDA in 0.9% saline with 0.2% ascorbic acid was injected into the DLS at a flow rate of 1 µl/min. Coordinates for the injection site were 0.8 mm anterior to bregma, 2.0 mm lateral to the midline, and 2.4 mm ventral to the pial surface. In the week following 6-OHDA lesion, all mice were monitored daily for excessive weight loss prior to resuming behavioral testing.

Apomorphine-induced rotational behavior

Apomorphine-induced rotations were performed as previously described[21]. Mice were habituated in separate 5-gallon buckets for 15 min and then received intraperitoneal (i.p.) injection of 0.5 mg/kg apomorphine (Sigma, cat# 1041008) prepared in 0.9% saline. Mice were recorded for 15 min to capture the total number of contralateral rotations. Mice that did not exhibit any rotations after apomorphine injection were excluded from this experiment. Contralateral rotations were analyzed using Ethovision XT (Noldus, Leesburg, VA). Arena sizes, trial settings, and detection settings were maintained constant for all mice across all weeks of behavioral testing.

Methods to deplete 17β−estradiol in mice

Systemic 17β-estradiol was depleted using two independent methods: (**i**) bilateral OVX and (**ii**) inhibition of aromatase (AROM) with letrozole. In both cases, mice were injected i.p. with either saline (control) or cytisine. An additional group of OVX mice were injected i.p. with 17β−estradiol. All mice were assayed for apomorphine-induced contralateral rotations before and after 6-OHDA lesion. The sections below describe detailed protocols for the two experiments to deplete 17β-estradiol.

OVX depletion

C57Bl6 female mice (2-3 months) received either an OVX or sham surgery. As a treatment, all mice received alternate day intraperitoneal (i.p.) injections of either 200 µl 0.9% saline, 0.2 mg/kg cytisine in 0.9% saline, or a combination of 0.2 mg/kg cytisine and 0.1 mg/kg 17β−estradiol in corn oil + 1% DMSO two weeks after OVX for the duration of the experiment. The mice were randomly separated into the following treatment groups: (**i**) sham-operated females treated with saline (Sal SO), (**ii**) sham-operated females treated with cytisine (Cyt SO), (**iii**) OVX females treated with saline (Sal OVX), (**iv**) OVX females treated with cytisine (Cyt OVX), or (**v**) OVX females treated with a combination of cytisine and 17β−estradiol (Cyt OVX + E2). Behavior assays were performed prior to OVX, prior to 6-OHDA lesion, and two weeks post 6-OHDA lesion.

Letrozole depletion

C57Bl6 female mice (2-3 months) were sorted into the following treatment groups: (**i**) saline-treated (Sal), (**ii**) cytisine-treated (Cyt), (**iii**) letrozole-treated (Let), or (**iv**) cytisine and letrozole-treated (Cyt + Let). One week prior to 6-OHDA lesion, the Sal and Let groups received alternate day i.p. injections of 100 µl of 0.9% saline, while the Cyt and Cyt + Let group received 0.2 mg/kg cytisine in 0.9% saline. All groups continued to receive either saline or cytisine for the remainder of the experiment. After 6-OHDA lesion, Sal and Cyt mice received dual injections of 100 µl of corn oil + 1% DMSO, while Let and Cyt + Let mice received 100 µl of 1 mg/kg letrozole diluted in corn oil + 1% DMSO. Apomorphine rotation behavioral assays were performed before and after 6-OHDA lesion.

Tissue Collection

After the final behavior assays were performed, all mice were sacrificed with isoflurane anesthesia and transcardially perfused with 1X phosphate-buffered saline (PBS) followed by 10% formalin. Following perfusion, the uterus and brain were extracted from each animal. Uterine weights were measured using precision balances. Extracted brains were placed in 10% formalin overnight at 4 °C followed by 30% sucrose until the time of sectioning. Using a Leica CM1850 cryostat (Leica, Deer Park, IL), 40 µm coronal sections containing the midbrain were obtained. All sections were collected in 0.01% sodium azide (Sigma, cat# S2002) and stored sequentially in 96 well plates to maintain the exact rostrocaudal positioning of the midbrain sections.

Quantification of SNc DA neuron loss

The extent of 6-OHDA induced SNc DA neurodegeneration was assessed by obtaining ratios of lesioned and unlesioned SNc tyrosine hydroxylase (TH) fluorescent intensities from mouse midbrain sections as previously described[21]. This method allows for the quantification of all functional compartments of SNc DA neurons, including extrasomatic neuronal components. Briefly, 10 midbrain sections were selected at 120 µm intervals from each mouse for TH immunostaining. Following a wash in PBS, sections were blocked and permeabilized in 10% normal goat serum (Abcam, ab7481) and 0.5% Triton X-100 rocking for 45 min at room temperature (RT). Sections were washed twice with PBS before incubation overnight at 4 °C with chicken anti-TH (1:2000, Abcam cat# ab76442) in 1% NGS + 0.05% Triton X-100. The next day sections were washed twice with PBS followed by incubation in goat anti-chicken AlexaFluor 594 (1:2000, Abcam, ab150176) for 1 h at RT.

For each midbrain section, rectangular 10 mm^2 regions of interest (ROIs) were drawn around the SNc on each side of the midbrain such that the lesioned and unlesioned SNc could be obtained in a single image. Each image contained a 20 µm thick optical z-stack and was acquired using an Olympus VS120 equipped with a 10x objective. Of the 10 immunostained midbrain sections, only 8 sections in which the SNc and VTA could be visually separated were selected for imaging. Imaging parameters were maintained across all sections and mice. Z-stacks were then sum projected using Fiji software and individual ROIs were manually drawn around the lesioned and unlesioned SNc with the polygon tool. Each ROI was thresholded to select TH^+ cell bodies and fibers to obtain integrated fluorescent intensities for each ROI. Fluorescent intensities across 8 midbrain sections per mouse for either the lesioned or unlesioned SNc were totaled and normalized to the maximum intensity value for each group. Ratios of lesioned to unlesioned SNc fluorescent intensities were compared between groups.

Quantification of glial fibrillary acid protein (GFAP), aromatase (AROM), and ionized calcium-binding adaptor molecule 1 (IBA1) staining

To assess the effects of 17β− estradiol depletion on astrocyte reactivity, brain-derived estrogen, and microglial activation, we respectively quantified GFAP, AROM, and IBA1 expression in mouse midbrains using immunofluorescence staining. To quantify intensity, 4 midbrain sections from mice in Experiment 1 were selected at 440 µm intervals between sections. Sections were washed in 1X PBS, blocked and permeabilized in 10% normal goat serum (Abcam, ab7481) and 0.5% Triton X-100 with rocking for 45 min at RT. Sections were washed twice with PBS before incubation overnight at 4 °C with rabbit anti-aromatase (1:2000, Abcam cat # ab18995), chicken anti-TH (1:2000, Abcam cat# ab76442), and mouse anti-GFAP (1:2000, Invitrogen cat# 14-9892-82) in 1% NGS + 0.05% Triton X-100. The next day, sections were washed twice with PBS followed by incubation in goat anti-rabbit AlexaFluor 488 (1:2000, Abcam cat# ab150077), goat anti-chicken AlexaFluor 594 (1:2000, Abcam cat# ab150176), and goat anti-mouse AlexaFluor 647 (1:2000, Abcam cat# ab150115) for 1 h at RT. In a separate staining procedure, sections were washed, blocked, and permeabilized in an identical manner, then incubated overnight at 4°C with rabbit anti-IBA1 (1:1000, Fujfilm Wako cat #019-19471), and chicken anti-TH (1:2000, Abcam cat# ab76442). The next day, sections were washed twice with PBS followed by incubation in goat anti-rabbit AlexaFluor 488 (1:2000, Abcam cat# ab150077) and goat anti-chicken AlexaFluor 594 (1:2000, Abcam cat# ab150176).

Two z-stacks from the lesioned and unlesioned SNc were acquired from each section using an Olympus FV3000 confocal microscope equipped with LED excitation at 488, 594 and 647 nm and a 60x oil objective lens. Each z-stack was composed of 25 optical sections with a step size of 0.49 µm. All imaging parameters were maintained across treatment groups and imaging days. Using Fiji, a max projection was made from each z-stack and a histogram range that subtracted background fluorescence was applied to each image. The same histogram range was used for all images. Images were then thresholded to select all the pixels in the image and the threshold was applied to the image to create a binary mask. The binary mask was then combined with the original image using the AND image calculator function in Fiji. The AND function results in an image containing only the pixels present in both images. SNc fluorescent intensities for GFAP, AROM, and IBA1 from AND images were obtained for each treatment group.

Statistics

Origin 2022 (OriginLab, Northampton, MA) was used for statistical analysis and creation of graphs. All data sets were first tested for normality. For comparisons between 2 treatment groups, normally distributed data were analyzed with two-sample t-tests. A two-way mixed design ANOVA was performed to determine the between subject effects of a fixed factor (treatment group) on body weight with a repeated measure designated as average body weight for a given week[22]. A one-way ANOVA test was performed to compare three or more treatment groups after 6-OHDA lesion[23]. Statistical significance was considered as $p < 0.05$. The types of statistical tests used are detailed in results, and sampling numbers for each experiment are detailed in each figure legend. Graphical elements depicting the mouse in Figs. 1 and 4 were created by the authors. The graphical element depicting apomorphine-induced contralateral rotations in Fig. 1d was created using Biorender.com under a license purchased by Texas A&M University, which includes publishing rights.

Results

Cytisine fails to reduce apomorphine-induced contralateral rotations in 6-OHDA lesioned mice with bilateral OVX

To determine if the depletion of systemically circulating 17β−estradiol could prevent neuroprotection by cytisine in 6-OHDA lesioned parkinsonian mice, bilateral OVX was performed in 2 – 3-month-old female mice. Sham-operated (SO) mice with intact ovaries were used as controls (Fig. 1a). Since OVX-induced depletion of circulating 17β−estradiol is known to cause an increase in body weight, along with a decrease in uterine weight[24], we compared whole body and uterine weights between control SO and OVX mice. Compared to SO mice, all OVX groups showed a significant 12% increase in body weight at two weeks post-OVX surgery, which persisted throughout the remainder of the experiment ($F_{(4,73)} = 5.57$, $p = 0.02$; two-way mixed design ANOVA) (Fig. 1b). Additionally, 5 weeks post-OVX, uterine weights were significantly reduced by ~80% in OVX mice without 17β−estradiol treatment when compared to SO mice. ($F_{(4,69)} = 12.4$, $p < 0.0001$; one-way ANOVA) (Fig. 1c). Notably, uterus weights of OVX mice with 17β−estradiol treatment did not change compared to SO mice. These data indicate the successful depletion of circulating 17β−estradiol in bilateral OVX mice and successful exogenous supplementation of 17β−estradiol via i.p. injection, which achieved biologically functional systemic levels of 17β-estradiol in OVX mice.

As shown in Fig. 1a, SO and OVX mice received alternate day i.p. injections of either 0.9% saline (Sal), 0.2 mg/kg cytisine (Cyt), or a combination of 0.2 mg/kg cytisine and 0.1 mg/kg 17β−estradiol starting in week 4, followed by a unilateral striatal lesion with stereotaxic injection of 6-OHDA into the dorsolateral striatum (DLS) in week 5. Following 6-OHDA striatal lesions, saline-treated sham-operated (Sal SO) mice showed a 12-fold increase in apomorphine rotations when compared to baseline from 6.5 ± 0.98 rotations in W1 to 87.1 ± 8.35 rotations in W7 ($F_{(1.03,19.62)} = 103.22$; $p = 2.4 \times 10^{-9}$; one-way repeated measures ANOVA) (Fig. 1e). Consistent with our prior findings[21], SO mice treated with cytisine (Cyt SO) showed significantly reduced apomorphine rotations when compared to Sal SO mice (Cyt SO: 63.84 ± 6.46 rotations; Sal SO: 87.1 ± 8.35 rotations, $p = 0.04$; two-sample t-test) (Fig. 1e). By contrast, when compared to Sal OVX mice, Cyt OVX mice demonstrated an increase in rotations after 6-OHDA lesion (Sal OVX: 56.8 ± 6.8 rotations; Cyt OVX: 83.4 ± 9.22 rotations, $p = 0.08$; two-sample t-test) (Fig. 1e). These data indicate that cytisine fails to reduce unilateral apomorphine rotational behavior in mice with depletion of circulating 17β-estradiol. It should be noted that Sal OVX mice demonstrated significantly reduced apomorphine rotations when compared to Sal SO mice (Sal SO: 87.1 ± 8.35 rotations; Sal OVX: 56.8 ± 6.8

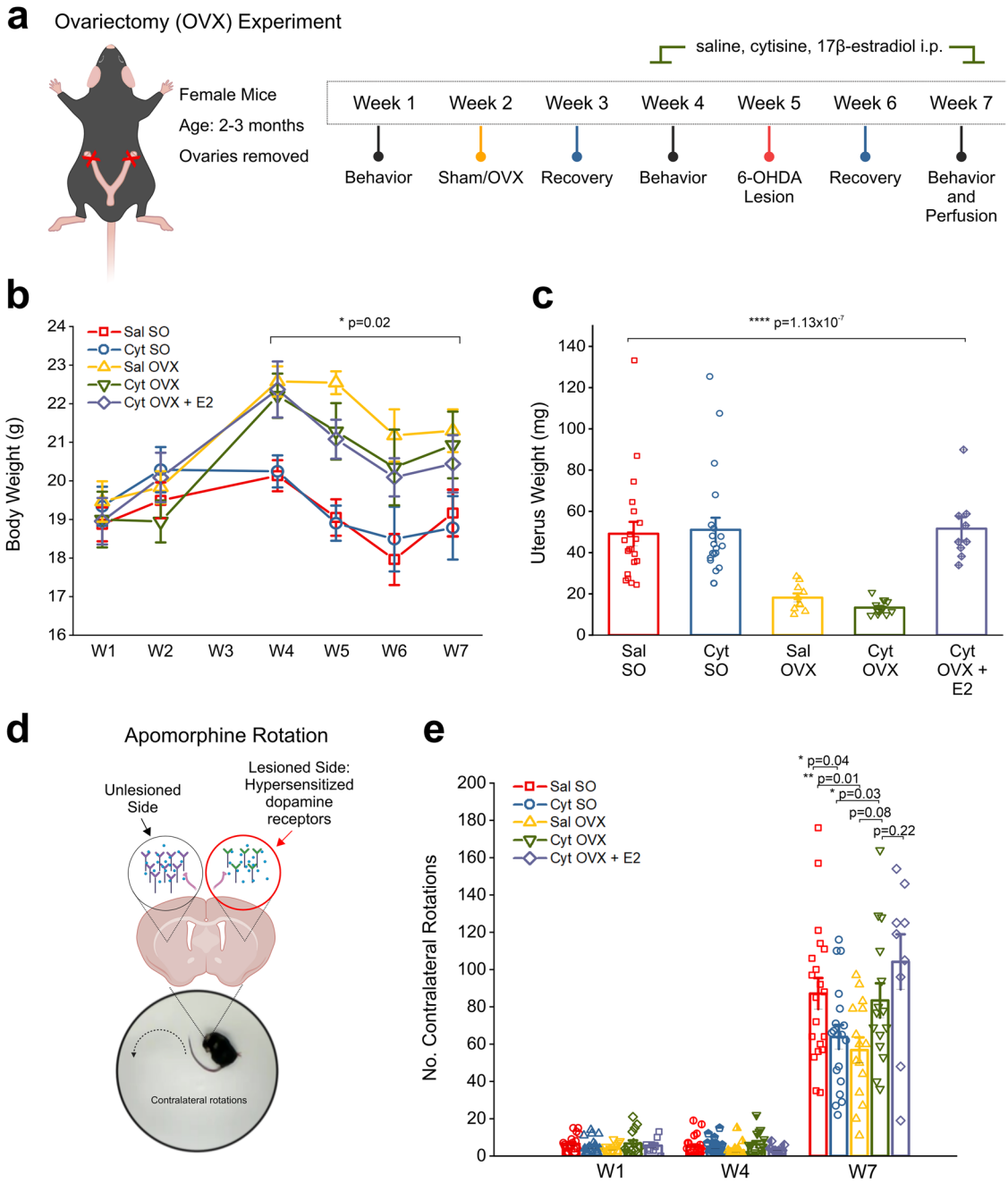

Fig. 1 | OVX induces long lasting changes to body, uterine weight, and apomorphine-induced contralateral rotations. a Schematic showing the protocol and timeline for OVX experiment in female mice. **b** Comparison of body weight changes across the experiment timeline for each treatment group. **c** Comparison of uterine weights collected at the end of the experiment, 5 weeks after OVX. **d** Schematic showing the rationale for apormophine-induced contralateral rotations that occurs due to hypersensitized dopamine receptors in the 6-OHDA lesioned DLS. **e** Bar graph showing the number of contralateral rotations counted in 15 min after i.p. injection with 0.5 mg/kg apomorphine for weeks 1, 4, and 7. Error bars are S.E.M. For panel b the *p* value was derived from a two-way mixed design ANOVA considering sham/OVX by time. For panel c, *p* values were derived from a one-way ANOVA test for all treatment groups. Comparison for increased rotations in W1-7 *p* value is derived from a one-way repeated measures ANOVA. For between group comparisons on W7 *p* values are based on two-sample t-tests $n = 20$ saline SO, $n = 19$ cytisine SO, $n = 15$ saline OVX, $n = 15$ cytisine OVX female mice, $n = 9$ cytisine OVX + E2 mice. Panel d was created using Biorender.com.

rotations, $p = 0.01$; two-sample t-test) (Fig. 1e), which suggests that OVX alone reduces apomorphine-induced contralateral rotational behavior in mice with unilateral 6-OHDA lesions in the striatum. Furthermore, exogenous supplementation of 17β−estradiol in cytisine-treated OVX mice (Cyt OVX + E2) did not reduce contralateral rotations when compared to cytisine-treated OVX mice without 17β−estradiol supplementation, and instead resulted in a non-significant increase in rotations (Cyt OVX: 83.4 ± 9.22 rotations; Cyt OVX + E2: 104.1 ± 14.8 rotations, $p = 0.22$; two-sample t-test) (Fig. 1e).

Cytisine does not prevent 6-OHDA-induced loss of SNc DA neurons in OVX mice

Having observed significant differences in contralateral apomorphine rotations among experimental groups (Fig. 1e), we sought to determine the extent to which cytisine and/or OVX treatment affects 6-OHDA-induced loss of SNc DA neurons. To do this, all mice were perfused in week 7 of the experimental protocol shown in Fig. 1a. Forty-micron midbrain sections were obtained along the rostrocaudal axis and immunostained for TH (Fig. 2a, b). To quantify the extent of midbrain SNc DA neuron loss for each of

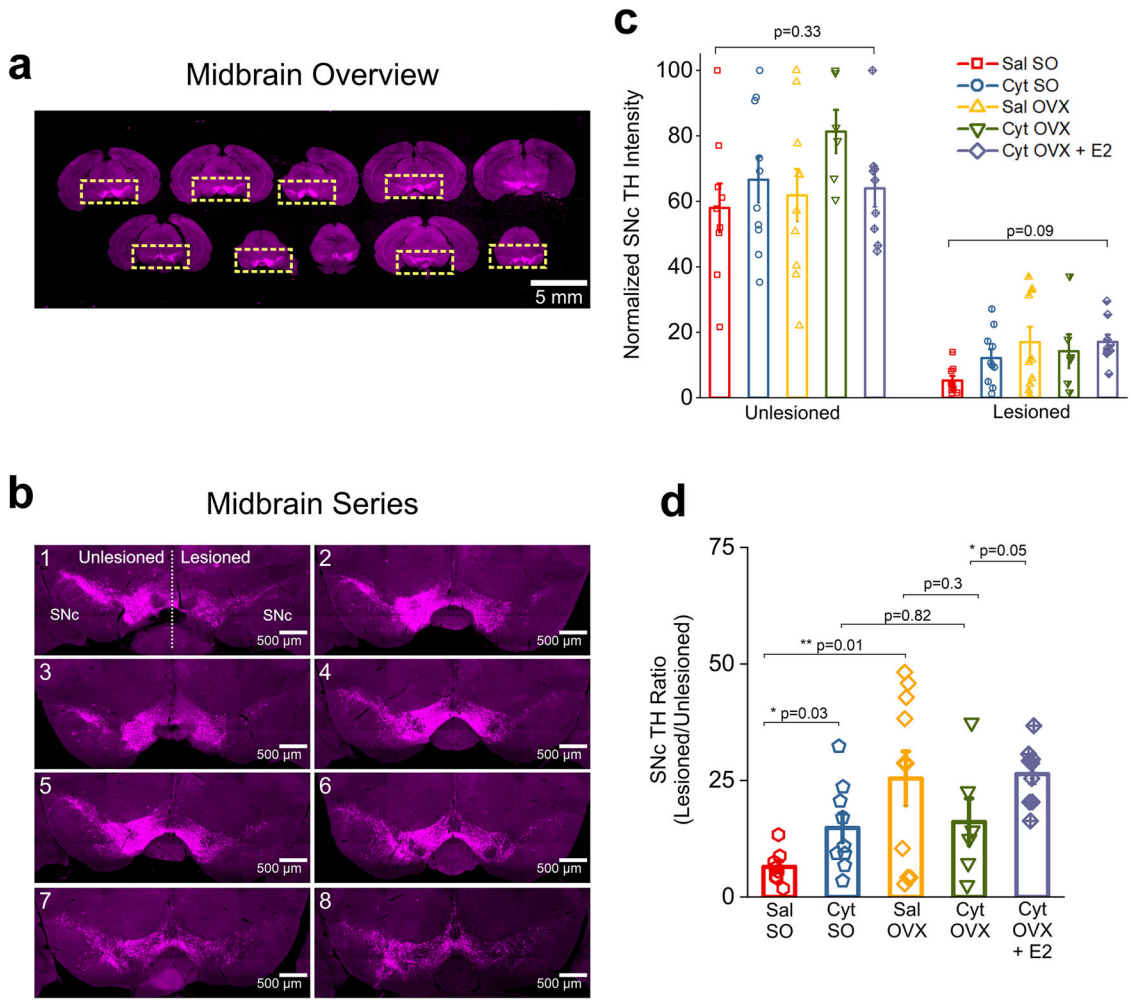

Fig. 2 | OVX does not reverse cytisine induced neuroprotection after 6-OHDA lesion. a Low magnification representative images of serial midbrain sections at 120 µm intervals. Only sections where the boundary between the SNc and VTA was clearly defined were selected for analysis. ROIs were manually demarcated such that the unlesioned and lesioned midbrain can be viewed in a single image. Scale bar = 5 mm. **b** Representative images of a midbrain series from a single mouse containing 8 TH labeled midbrain sections used for analysis. Scale bar = 500 µm. **c** Bar graphs comparing total TH intensity in either the unlesioned or lesioned SNc for all treatment groups. Each data point is the sum of TH intensity measured for either the unlesioned or lesioned SNc in 8 images per mouse. **d** Bar graphs comparing TH intensity ratios for all treatment groups. Each data point is the total lesioned SNc TH intensity by the total unlesioned SNc TH intensity. Error bars are S.E.M. For panel c, the *p* values for the unlesioned and lesioned comparisons are derived from a one-way ANOVA comparing each treatment group. For panel **d**, *p* values are derived from two-sample t-tests. $n = 9$ saline SO, $n = 10$ cytisine SO, $n = 10$ saline OVX, $n = 6$ cytisine OVX female mice, and $n = 9$ cytisine OVX + E2 mice.

these mice, we obtained integrated TH intensities for the lesioned and unlesioned SNc (Fig. 2c) and lesioned / unlesioned SNc TH integrated intensity ratios (Fig. 2d) for all mice in each experimental group as described in methods. We found that the ratio of lesioned to unlesioned SNc TH intensity was significantly higher in Cyt SO mice when compared to Sal SO (Sal SO, TH ratio: 0.06 ± 0.012 and Cyt SO, TH ratio: 0.15 ± 0.031, $p = 0.03$; two-sample t-test) (Fig. 2d). These data confirm our previous finding that cytisine alone exerts a neuroprotective effect on 6-OHDA lesioned SNc DA neurons in female mice with intact ovaries[21].

By contrast, when compared to Sal OVX mice, Cyt OVX mice failed to show a significant increase in SNc TH ratio (Sal OVX, TH ratio: 0.24 ± 0.05 and Cyt OVX, TH ratio: 0.16 ± 0.05, $p = 0.3$; two-sample t-test) (Fig. 2d). However, when exogenous 17β−estradiol was administered in combination with cytisine to OVX mice, there was a significant increase in SNc TH ratio in comparison to OVX mice treated with cytisine alone (Cyt OVX, TH ratio: 0.16 ± 0.05 and Cyt OVX + E2, TH ratio: 0.26 ± 0.02, $p = 0.05$, two-sample t-test) (Fig. 2d). Taken together, these data show that OVX-induced depletion of circulating 17β−estradiol prevents the neuroprotective effect of cytisine in midbrain SNc DA neurons, and that exogenously administered 17β-estradiol rescues this neuroprotective effect. It should be noted that when compared to Sal SO mice, Sal OVX mice showed a significant 2.7-fold increase in TH intensity ratio after 6-OHDA lesion (Sal SO, TH ratio: 0.06 ± 0.012 and Sal OVX, TH ratio: 0.24 ± 0.05, $p = 0.01$; two-sample t-test) (Fig. 2d), which suggests an additional neuroprotective effect of OVX alone.

Cytisine does not decrease astrocyte reactivity in the 6-OHDA lesioned SNc of OVX mice

Increased astrocyte reactivity occurs as a consequence of ongoing DA neurodegeneration within the SNc, which can accelerate the neurodegenerative process in PD[25–27]. Based on this rationale, we sought to quantify changes in GFAP intensity within the 6-OHDA-lesioned SNc of mice from experimental groups Sal SO, Cyt SO, Sal OVX and Cyt OVX. Midbrain sections were stained for GFAP and confocal images of the lesioned SNc were obtained for quantification of GFAP intensity in each mouse (Fig. 3a). Compared to Sal SO mice, Cyt SO mice showed a significant decrease in GFAP intensity within the lesioned SNc (Sal SO, GFAP intensity: 14.90 ± 1.16 and Cyt SO, GFAP Intensity: 7.36 ± 1.65, $p = 0.03$; one-way ANOVA with post-hoc Tukey test) (Fig. 3b), which correlates with the neuroprotective effect of cytisine shown in Fig. 2D. However, when compared to Sal SO mice, Sal OVX mice showed no significant difference in

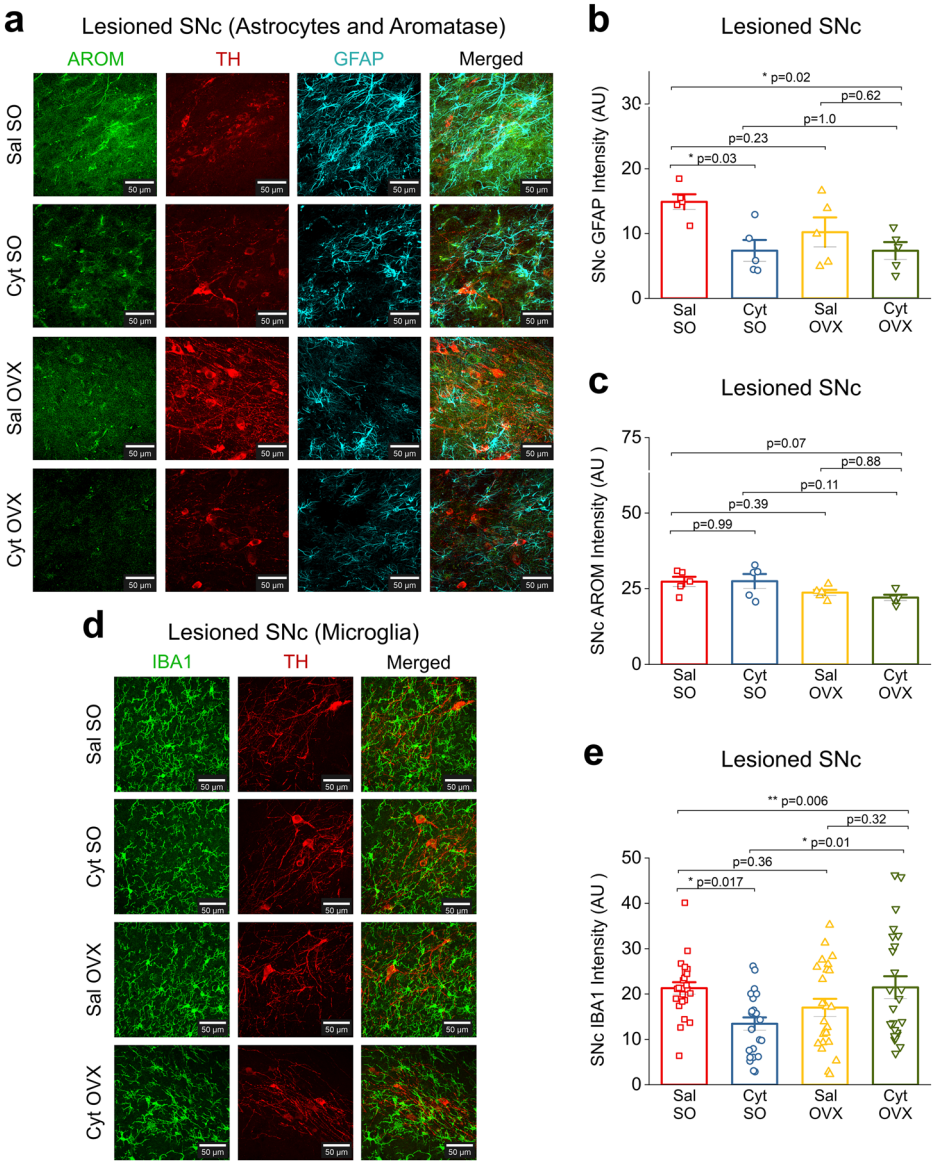

Fig. 3 | Cytisine neuroprotection in OVX mice is independent of glial derived estrogen.
a Representative confocal images from the lesioned SNc across treatment groups for AROM and GFAP immunostaining. All sections were stained for AROM (green), TH (red), and GFAP (cyan). Scale bar = 25 µm. **b** Bar graph comparing total GFAP intensity in the lesioned SNc for all treatment groups **c** Bar graph comparing total AROM intensity in the lesioned SNc for all treatment groups. **d** Representative confocal images from the lesioned SNc across treatment groups for IBA1 immunostaining. All sections were stained for IBA1 (green) and TH (red). Scale bar = 25 µm. **e** Bar graph comparing IBA1 intensity in the lesioned SNc for all treatment groups. Each data point is the average of either GFAP, AROM, or IBA1 intensity measured from 4 images for the lesioned SNc. Error bars are S.E.M. *p* values are derived from a one-way ANOVA and Tukey post hoc comparisons between treatment groups. For GFAP and AROM staining, $n = 5$ for each group. For IBA1 staining, $n = 4$ for each group.

GFAP intensity (Sal SO, GFAP intensity: 14.90 ± 1.16 and Sal OVX, GFAP intensity: 10.22 ± 2.27, $p = 0.23$; one-way ANOVA with post-hoc Tukey test) (Fig. 3b). Importantly, when compared to Sal OVX mice, Cyt OVX mice did not show a further decrease in GFAP intensity within the lesioned SNc (Sal OVX, GFAP intensity: 10.22 ± 2.27 and Cyt OVX, GFAP intensity: 7.35 ± 1.34, $p = 0.62$; one-way ANOVA with post-hoc Tukey test) (Fig. 3b). This finding provides additional evidence that the neuroprotective effect of cytisine in the SNc is enhanced by circulating 17β-estradiol via a reduction of 6-OHDA-induced astrocyte reactivity in the SNc.

Brain-derived 17β-estradiol does not contribute to cytisine-mediated neuroprotection in the 6-OHDA lesioned SNc

Results thus far show that depletion of circulating 17β-estradiol via OVX results in a loss of neuroprotection by cytisine. Cells in the brain are steroidogenic and express aromatase (AROM), which is the primary cytochrome P450 enzyme (CYP19A1) that synthesizes 17β-estradiol in the brain[28]. Therefore, to determine the contribution of brain-derived 17β-estradiol to cytisine-mediated neuroprotection, we sought to quantify changes in AROM expression in the lesioned SNc of mice from all experimental groups *viz.* Sal SO, Cyt SO, Sal OVX and Cyt OVX. Midbrain sections from mice in each experimental group were immunostained for AROM (Fig. 3a) and AROM intensity was quantified from confocal images of the lesioned SNc in these mice as described in the methods. Midbrain AROM intensity analysis revealed that neither cytisine treatment nor OVX resulted in significant changes in aromatase expression (Sal SO, AROM intensity: 27.29 ± 1.62; Cyt SO, AROM intensity: 27.44 ± 2.38; Sal OVX, AROM intensity: 23.66 ± 0.92, Cyt OVX, AROM intensity: 22.02 ± 0.93, $p = 0.07$; one-way ANOVA) (Fig. 3c). These data suggest that the loss of cytisine-mediated neuroprotection in OVX mice stems from a depletion of circulating and not brain-derived 17β-estradiol.

Cytisine does not decrease microglial activation in the 6-OHDA lesioned SNc of OVX mice

Microglial activation plays a critical role in PD. This is demonstrated by increased activation in the SNc of various PD models and human PD midbrain samples[29,30], as well as the finding that reactive microglia contribute to PD pathogenesis[31]. We therefore sought to determine the effect of cytisine on microglial activation by quantifying IBA1 fluorescence intensity in the 6-OHDA-lesioned SNc of Sal SO, Cyt SO, Sal OVX and Cyt OVX mice. Midbrain sections were stained for IBA1 and confocal images of the lesioned SNc were obtained for quantification of IBA1 intensity in each mouse (Fig. 3d). Compared to Sal SO mice, Cyt SO mice showed a

significant decrease in IBA1 intensity within the lesioned SNc (Sal SO, IBA1 intensity: 21.29 ± 1.32 and Cyt SO, IBA1 Intensity: 13.44 ± 1.41 $p = 0.017$; one-way ANOVA with post-hoc Tukey test) (Fig. 3e), which correlates with the neuroprotective effect of cytisine shown in Fig. 2d and the reduction in astrocyte reactivity shown in Fig. 3b. Notably, in comparison to Sal OVX mice, Cyt OVX mice did not show a decrease in IBA1 intensity within the lesioned SNc (Sal OVX, IBA1 intensity: 17.02 ± 1.93 and Cyt OVX, IBA1 intensity: 21.46 ± 2.46, $p = 0.32$; one-way ANOVA with post-hoc Tukey test) (Fig. 3e). This finding suggests that the neuroprotective effect of cytisine may be mediated in part by a reduction in SNc microglial activation, which occurs only in the presence of systemically circulating 17β-estradiol.

Depletion of 17β−estradiol with the AROM inhibitor letrozole prevents cytisine-induced neuroprotection of SNc DA neurons

We have shown that the depletion of systemically circulating 17β−estradiol via OVX prevents cytisine-mediated neuroprotection of SNc DA neurons (Figs. 1–3). However, when compared to mice with intact ovaries, we find that OVX alone exerts neuroprotection in the SNc DA neurons of 6-OHDA lesioned mice (Fig. 2d). Based on these findings, we sought to assess cytisine neuroprotection using systemic AROM inhibition as a model of 17β−estradiol depletion, which would reduce the long-term compensatory effects that are seen with OVX.

We administered 1 mg/kg of the AROM inhibitor, letrozole (Let) i.p to mice on alternate days for two weeks, starting one day after striatal 6-OHDA lesion (Fig. 4a). The four experimental groups of 6-OHDA lesioned mice were as follows: (**i**) 6-OHDA lesioned mice with only i.p. saline (Sal), (**ii**) 6-OHDA-lesioned mice with only cytisine 0.2 mg/kg i.p., (Cyt) (**iii**) 6-OHDA lesioned mice with only 1 mg/kg letrozole i.p. (Let), and (**iv**) 6-OHDA lesioned mice with 1 mg/kg of letrozole and 0.2 mg/kg cytisine i.p. (Cyt + Let). We found that when compared to saline-treated mice, Let treatment did not result in a significant difference in body or uterus weight ($p = 0.99$, one-way ANOVA with post-hoc Tukey test) (Fig. 4b, c), suggesting minimal long-term compensatory changes following Let treatment. After 6-OHDA lesions, all four groups of mice were compared for apomorphine-induced rotations in week 4 (Fig. 4d). Similar to the Saline SO and Cytisine SO groups in Fig. 1e, we found a significant decrease in the number of contralateral rotations between the saline and cytisine-treated groups with no letrozole treatment (Sal: 105.8 ± 23.0 rotations; Cyt: 31.9 ± 9.5 rotations, $p = 0.003$; two-sample t-test) (Fig. 4d). Importantly, among letrozole-treated saline and cytisine mice, there was no significant difference in number of rotations (Let: 77.38 ± 12.70 rotations; Cyt + Let: 82.13 ± 8.32 rotations, $p = 0.76$; two-sample t-test) (Fig. 4d). Additionally, we observed no significant difference in number of rotations between the saline and letrozole-treated groups (Sal: 105.8 ± 23.0 rotations; Let: 77.38 ± 12.70 rotations, $p = 0.27$). We then stained midbrain sections from all mice to determine DA neuron survival after 6-OHDA lesion (Fig. 4e). Among mice with no letrozole treatment, TH intensity ratios were increased in cytisine-treated mice when compared to saline-treated mice (Sal, TH ratio: 0.13 ± 0.04; Cyt, TH ratio: 0.21 ± 0.02, $p = 0.08$, two-sample t-test) (Fig. 4g). In contrast, no increase was detected after cytisine treatment when TH intensity ratios were compared between Let and Cyt + Let groups (Let, TH ratio: 0.21 ± 0.05; Let + Cyt TH ratio: 0.14 ± 0.04, $p = 0.21$, two-sample t-test) (Fig. 4g). Additionally, we observed no significant difference in TH intensity ratios between the saline and letrozole-treated groups (Sal: 0.13 ± 0.04; Let: 0.21 ± 0.05, $p = 0.21$) (Fig. 4g). Together, these data demonstrate that the acute depletion of 17β-estradiol in female mice with intact ovaries also prevents cytisine-mediated neuroprotection of 6-OHDA lesioned SNc DA neurons.

Discussion

In this study, we determine the extent to which the smoking cessation drug cytisine depends on systemically circulating 17β-estradiol for neuroprotection against 6-OHDA-induced SNc DA neuron loss in female mice. To do this, we employ two different mouse models that deplete circulating 17β-estradiol in 6-OHDA lesioned female mice: (**i**) bilateral OVX, and (**ii**) acute pharmacological inhibition of AROM with letrozole. In each of these models, we show that pre-treatment with cytisine along with depletion of systemically circulating 17β-estradiol results in the loss of cytisine-mediated neuroprotection in SNc DA neurons (Fig. 2d–g). Importantly, the current study recapitulates our previous finding that cytisine exerts neuroprotection in female mice with intact ovaries (Fig. 2d)[21].

The use of two types of models to deplete systemically circulating 17β-estradiol is an important aspect of this study because this approach addresses the possibility of model-specific idiosyncrasies that can lead to incorrect interpretation of data. One such idiosyncrasy is that when compared to sham-operated mice with intact ovaries, OVX mice with unilateral striatal 6-OHDA lesions display significantly reduced contralateral rotations with apomorphine, which is indicative of neuroprotection (Fig. 1e). This effect could partly be explained by OVX-mediated compensatory changes in the striatum, specifically a decrease in the expression of striatal dopamine type 1 (D1) receptors[32,33]. Apomorphine rotations are induced by the activation of hypersensitive dopamine receptors in striatal medium spiny neurons (Fig. 1d), with the number of rotations providing an indirect measure of SNc DA neuron loss after unilateral striatal lesion[34,35]. Thus, an OVX-induced compensatory decrease in striatal D1 receptors likely contributes to reducing the total number of contralateral rotations with apomorphine. Extending these data, we find that pre-treatment of OVX mice with cytisine causes a significant increase in apomorphine rotations when compared to mice with OVX alone (Fig. 1e). Our interpretation of this result is that chronic cytisine treatment upregulates α4β2* nAChRs (* indicates additional uncharacterized nAChR subunits in the ion channel pentamer) in SNc DA terminals within the striatum, which would in turn increase the basal release of dopamine in the striatum[36]. Therefore, it follows that the activation of striatal D1 receptors by a cytisine-induced increase in basal dopamine release on the lesioned side would generally increase apomorphine-induced contralateral rotations in cytisine-treated OVX mice with unilateral loss of SNc DA neurons.

In addition to reducing apomorphine rotations, we show that OVX alone exerts a neuroprotective effect in 6-OHDA-lesioned SNc DA neurons of mice (Fig. 2d). Previous studies have shown that OVX in mice robustly alters GFAP promoter activity in the central nervous system following ischemia, suggesting that systemically circulating 17β-estradiol can exert an effect on astrocyte reactivity during brain injury[37]. However, our data has shown that in the context of 6-OHDA-induced DA neuron loss, OVX results in a small, but non-significant decrease in GFAP intensity, suggesting that astrocytes might play a relatively small role in our experimental mouse models. We also observed that cytisine decreases GFAP intensity in intact female mice, but not in OVX mice. In this context, one future question that remains to be explored is the extent to which cytisine can directly alter SNc astrocyte function during the process of neurodegeneration. For example, cytisine could cause astrocytes to increase their secretion of antioxidants[38], mitigate mitochondrial damage in SNc DA neurons[39], or increase phagocytosis of abnormal protein aggregates[40]. The idea that a decrease in astrocyte reactivity can be specifically neuroprotective in the SNc is supported by our prior demonstration that astrocyte processes in the SNc completely envelop DA neuron somata[41], which places SNc astrocytes in a unique morphological position to exert direct effects on SNc DA neuron survival. In addition to astrocytes, we investigated the effect of cytisine on microglial activation in the 6-OHDA-lesioned SNc in intact and OVX mice. Interestingly, cytisine treatment in intact females reduced microglial activation (Fig. 3e), suggesting that cytisine may mediate neuroprotection, in part, by reducing the extent of microglial activation. This notion is supported by previously published reports that nAChR agonists and 17β-estradiol inhibit microglial activation in mice[42,43], supporting the idea that both molecules may work synergistically to modulate microglial reactivity. Importantly, these findings suggest that in the presence of systemically circulating 17β-estradiol, cytisine may reduce the pathological activation of multiple glial cells.

Cytisine-treated OVX mice did not demonstrate a change in SNc DA neuron loss when compared to intact mice treated with cytisine (Fig. 2d). Furthermore, when cytisine-treated OVX mice were exogenously administered 17β-estradiol, these mice showed a significant increase in the

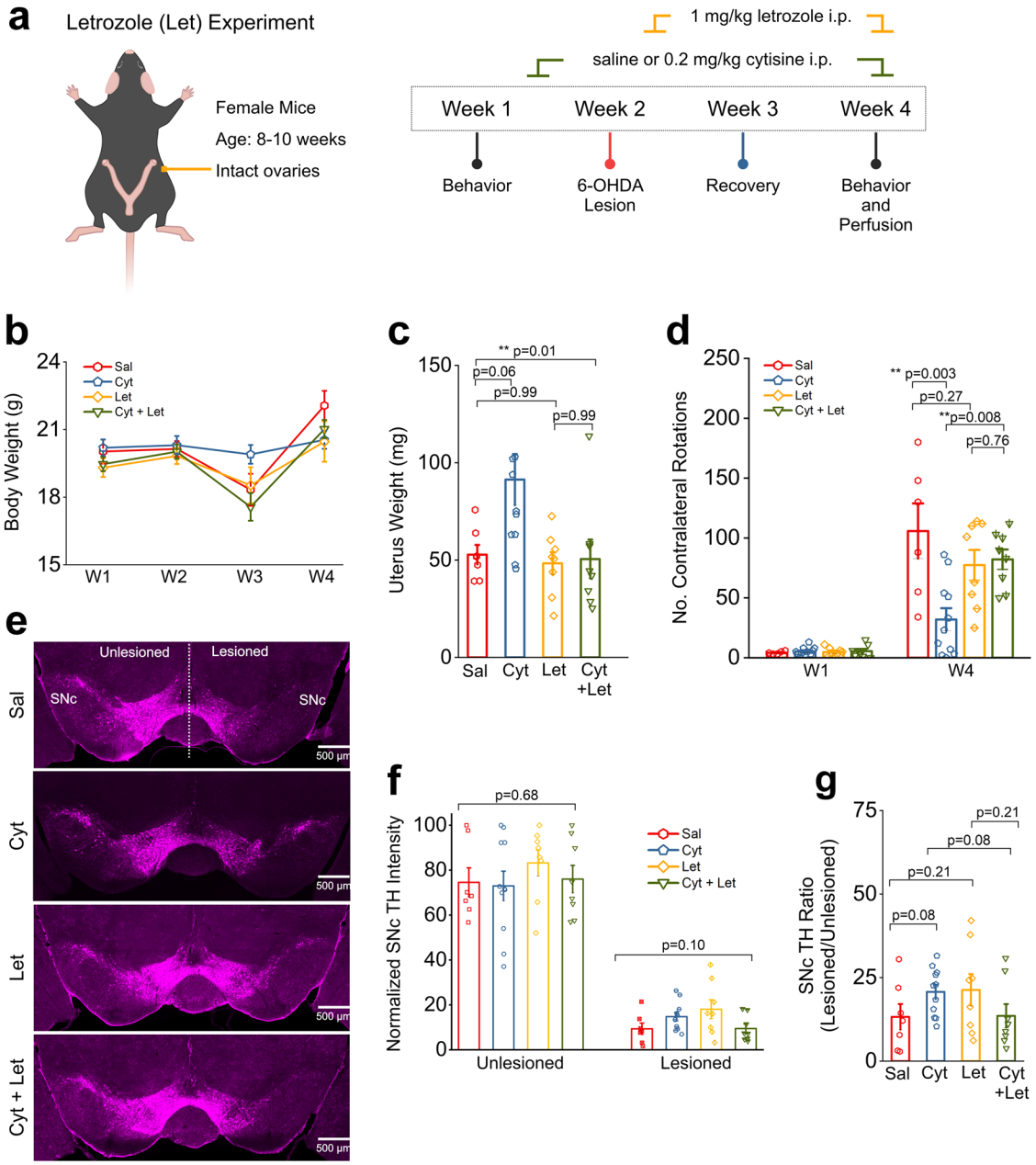

Fig. 4 | Cytisine neuroprotection is reversed by aromatase inhibition. a Schematic of protocol for behavior assays. **b** Comparison of body weight changes across the experiment timeline for each treatment group. **c** Comparison of uterine weights collected at the end of the experiment. **d** Bar graph showing the number of contralateral rotations counted in 15 min after i.p. injection with 0.5 mg/kg apomorphine for weeks 1 and 4. **e** Representative images of a single midbrain section from each treatment group. Scale bar = 500 µm (**f**) Bar graphs comparing total TH intensity in either the unlesioned or lesioned SNc for all treatment groups. Each data point is the sum of TH intensity measured for either the unlesioned or lesioned SNc in 8 images per mouse. **g** Bar graphs comparing TH intensity ratios for all treatment groups. Error bars are S.E.M. For panel c, the *p* values were derived from a one-way ANOVA test for all treatment groups. For panels d and g, the *p* values are based on two-sample t-tests. For panel f, the *p* values are derived from a one-way ANOVA comparing each treatment group in the unlesioned or lesioned SNc. $n = 7$ saline mice, $n = 7$ cytisine mice, $n = 8$ letrozole mice (let), and $n = 8$ cytisine + letrozole mice (cyt+let).

neuroprotective effect of cytisine (Fig. 2d). We interpret these data as evidence for a negative correlation between systemic 17β-estradiol depletion and the neuroprotective effect of cytisine in female mice. One plausible explanation for this could be that 17β-estradiol is necessary for the expression, binding, function, stabilization and chaperoning of nAChRs from the ER[44]. Indeed, 17β-estradiol has been shown to bind to a specific portable sequence motif in the C-terminal domain of α4 nAChR subunits[45,46]. In this context, future studies will assess the effect of 17β-estradiol depletion on cytisine-mediated nAChR chaperoning and ERES upregulation in SNc DA neurons. It is also important to note that contrary to exogenously administered 17β-estradiol, physiologic estrogen levels fluctuate throughout the mouse estrous cycle. Therefore, it is likely that constant, exogenous 17β-estradiol supplementation co-administered with cytisine is capable of exerting robust neuroprotection.

It should be noted that OVX results in a 70 to 80% loss of TH content in the SNc after 6-OHDA lesion, which is not attenuated by the pretreatment of OVX mice with cytisine (Fig. 2d). This suggests that the neuroprotective effect of cytisine is enhanced by systemically circulating 17β-estradiol. However, it is also possible that 6-OHDA lesions along with OVX and/or cytisine can upregulate brain-derived AROM, thereby causing neuroprotection by increasing local synthesis of 17β-estradiol within the SNc. We rule out this possibility by showing that OVX alone does not alter AROM

expression in the SNc when compared to mice with intact ovaries (Fig. 3c). Furthermore, cytisine does not significantly alter the expression of AROM in SO or OVX groups. Based on these data, we infer that when compared to OVX only mice, the observed loss of cytisine-mediated SNc neuroprotection by cytisine in the background of OVX is due to depletion of systemically circulating 17β−estradiol rather than changes in the production of brain-derived 17β−estradiol.

Another notable finding was that in comparison to Cyt OVX mice, Cyt OVX + E2 mice demonstrated increased apomorphine-induced contralateral rotations (Fig. 1e). This finding was surprising given that in both OVX and Let experiments, mice with intact endogenous 17β-estradiol production demonstrate cytisine-mediated neuroprotection and a reduction in apomorphine-induced rotations. Given that treatment of Cyt OVX mice with 17β-estradiol resulted in a protective effect on SNc DA neuron loss (Fig. 2d), it is likely that this increased rotational behavior is due to altered dopaminergic dynamics in other PD-relevant brain regions, such as the DLS. Indeed, multiple studies have demonstrated that treatment of female OVX rats with estrogen enhances dopamine release in the DLS, and that exogenous estrogen can also potentiate amphetamine-induced striatal dopamine release and rotational behavior[47,48]. Exogenous administration of 17β-estradiol in the Cyt OVX + E2 group is limited in its ability to closely mimic temporal fluctuations in circulating estrogen, which occur in female mice with an intact estrous cycle. Therefore, it is likely that constant administration of 17β-estradiol in Cyt + OVX mice results in altered DLS dopaminergic neurotransmission which may not occur in female mice with intact 17β-estradiol production.

The fact that OVX results in a neuroprotective effect in the lesioned SNc motivated us to employ a second model for 17β−estradiol depletion using letrozole, which is an AROM inhibitor. The absence of an abnormal increase in body weight or a decrease in uterine weight (Fig. 4b, c), as well as a lack of changes in apomorphine rotations (Fig. 4d) in letrozole-treated mice compared to saline-treated mice, supports our rationale that the strategy of acutely depleting 17β−estradiol immediately after 6-OHDA lesion mitigates long-term compensatory effects in mice. In control 6-OHDA mice given the corn oil vehicle, cytisine treatment resulted in a reduction in apomorphine-induced rotations (Fig. 4d) and an increased TH intensity ratio in the SNc (Fig. 4g). Importantly, in a background of letrozole-induced acute 17β-estradiol depletion, we found that cytisine fails to exert similar neuroprotective effects in SNc DA neurons (Fig. 4d – g). Taken together, based on our findings that cytisine exerts neuroprotection in mice with intact ovaries, but does not exert additional neuroprotection in OVX or letrozole-treated mice, we conclude that the neuroprotective effect of cytisine is mediated by systemically circulating 17β-estradiol in 6-OHDA lesioned female mice.

One limitation of this study is that we do not delineate downstream mechanisms by which circulating 17β-estradiol can act in combination with cytisine to prevent the loss of SNc DA neurons. In light of our previous study, it is likely that 17β-estradiol exerts neuroprotection by inhibiting the expression of the pro-apoptotic ER stress molecule, CHOP[21]. However, other downstream neuroprotective mechanisms such as ERES upregulation via 17β-estradiol-mediated chaperoning of nAChRs or direct genetic / epigenetic effects of estrogen in SNc DA neurons cannot be ruled out as potential mechanisms for the combined neuroprotective effects of 17β-estradiol and cytisine in female mice. Regardless of the downstream mechanism(s) involved, the current study bolsters our view that the smoking cessation drug cytisine prevents SNc DA neurons loss by acting in combination with circulating 17β-estradiol, and can therefore be regarded as a potential neuroprotective drug for pre-menopausal women with PD. In future studies, we will assess the extent to which a combination of cytisine along with systemically administered estrogen analogues that more closely mimic physiological estrogen fluctuations can exert neuroprotection in SNc DA neurons of male parkinsonian mice.

Data availability

The datasets used and/or analyzed during the current study are available from the corresponding author on reasonable request.

Received: 21 March 2024; Accepted: 22 November 2024;
Published online: 03 January 2025

References

1. Ritz, B. et al. Pooled analysis of tobacco use and risk of Parkinson disease. *Arch. Neurol.* **64**, 990–997 (2007).
2. Chen, H. et al. Smoking duration, intensity, and risk of Parkinson disease. *Neurology* **74**, 878–884 (2010).
3. Li, X., Li, W., Liu, G., Shen, X. & Tang, Y. Association between cigarette smoking and Parkinson's disease: A meta-analysis. *Arch. Gerontol. Geriatr.* **61**, 510–516 (2015).
4. Yang, F. et al. Moist smokeless tobacco (Snus) use and risk of Parkinson's disease. *Int J. Epidemiol.* **46**, 872–880 (2017).
5. Sallette, J. et al. Nicotine upregulates its own receptors through enhanced intracellular maturation. *Neuron* **46**, 595–607 (2005).
6. Kuryatov, A., Luo, J., Cooper, J. & Lindstrom, J. Nicotine acts as a pharmacological chaperone to up-regulate human alpha4beta2 acetylcholine receptors. *Mol. Pharm.* **68**, 1839–1851 (2005).
7. Srinivasan, R. et al. Pharmacological chaperoning of nicotinic acetylcholine receptors reduces the endoplasmic reticulum stress response. *Mol. Pharm.* **81**, 759–769 (2012).
8. Henderson, B. J. et al. Nicotine exploits a COPI-mediated process for chaperone-mediated up-regulation of its receptors. *J. Gen. Physiol.* **143**, 51–66 (2014).
9. Srinivasan, R., Henderson, B. J., Lester, H. A. & Richards, C. I. Pharmacological chaperoning of nAChRs: a therapeutic target for Parkinson's disease. *Pharm. Res.* **83**, 20–29 (2014).
10. Srinivasan, R. et al. Nicotine up-regulates alpha4beta2 nicotinic receptors and ER exit sites via stoichiometry-dependent chaperoning. *J. Gen. Physiol.* **137**, 59–79 (2011).
11. Srinivasan, R. et al. Forster resonance energy transfer (FRET) correlates of altered subunit stoichiometry in cys-loop receptors, exemplified by nicotinic alpha4beta2. *Int J. Mol. Sci.* **13**, 10022–10040 (2012).
12. Srinivasan, R. et al. Smoking-Relevant Nicotine Concentration Attenuates the Unfolded Protein Response in Dopaminergic Neurons. *J. Neurosci.* **36**, 65–79 (2016).
13. Costa, C. A. D., Manaa, W. E., Duplan, E. & Checler, F. The Endoplasmic Reticulum Stress/Unfolded Protein Response and Their Contributions to Parkinson's Disease Physiopathology. *Cells* **9** (2020).
14. Ren, H., Zhai, W., Lu, X. & Wang, G. The Cross-Links of Endoplasmic Reticulum Stress, Autophagy, and Neurodegeneration in Parkinson's Disease. *Front Aging Neurosci.* **13**, 691881 (2021).
15. Lemay, S. et al. Poor tolerability of a transdermal nicotine treatment in Parkinson's disease. *Clin. Neuropharmacol.* **26**, 227–229 (2003).
16. Villafane, G. et al. Chronic high dose transdermal nicotine in Parkinson's disease: an open trial. *Eur. J. Neurol.* **14**, 1313–1316 (2007).
17. Villafane, G. et al. High-dose transdermal nicotine in Parkinson's disease patients: a randomized, open-label, blinded-endpoint evaluation phase 2 study. *Eur. J. Neurol.* **25**, 120–127 (2018).
18. Ma, C., Liu, Y., Neumann, S. & Gao, X. Nicotine from cigarette smoking and diet and Parkinson disease: a review. *Transl. Neurodegener.* **6**, 18 (2017).
19. Charbonneau, P. F. & Damier, P. Nicotine in Parkinson's Disease - a Therapeutic Track Gone up in Smoke? *NEJM Evid.* **2**, EVIDe2300167 (2023).
20. De Santi, O., Orellana, M., Di Niro, C. A. & Greco, V. Evaluation of the effectiveness of cytisine for the treatment of smoking cessation: A systematic review and meta-analysis. *Addiction* **119**, 649–663 (2024).
21. Zarate, S. M. et al. Cytisine is neuroprotective in female but not male 6-hydroxydopamine lesioned parkinsonian mice and acts in combination with 17-beta-estradiol to inhibit apoptotic endoplasmic reticulum stress in dopaminergic neurons. *J. Neurochem* **157**, 710–726 (2021).

22. Ato Garcia, M., Vallejo Seco, G. & Palmer Pol, A. The two-way mixed model: a long and winding controversy. *Psicothema* **25**, 130–136 (2013).
23. Kim, H. Y. Statistical notes for clinical researchers: A one-way repeated measures ANOVA for data with repeated observations. *Restor. Dent. Endod.* **40**, 91–95 (2015).
24. Cavalcanti-de-Albuquerque, J. P. et al. Role of estrogen on skeletal muscle mitochondrial function in ovariectomized rats: a time course study in different fiber types. *J. Appl Physiol. (1985)* **116**, 779–789 (2014).
25. Booth, H. D. E., Hirst, W. D. & Wade-Martins, R. The Role of Astrocyte Dysfunction in Parkinson's Disease Pathogenesis. *Trends Neurosci.* **40**, 358–370 (2017).
26. Kim, S., Pajarillo, E., Nyarko-Danquah, I., Aschner, M. & Lee, E. Role of Astrocytes in Parkinson's Disease Associated with Genetic Mutations and Neurotoxicants. *Cells* **12**, (2023).
27. Ozoran, H. & Srinivasan, R. Astrocytes and Alpha-Synuclein: Friend or Foe? *J. Parkinsons Dis.* **13**, 1289–1301 (2023).
28. Azcoitia, I., Mendez, P. & Garcia-Segura, L. M. Aromatase in the Human Brain. *Androg. Clin. Res Ther.* **2**, 189–202 (2021).
29. Doorn, K. J. et al. Microglial phenotypes and toll-like receptor 2 in the substantia nigra and hippocampus of incidental Lewy body disease cases and Parkinson's disease patients. *Acta Neuropathol. Commun.* **2**, 90 (2014).
30. Thi Lai, T. et al. Microglial inhibition alleviates alpha-synuclein propagation and neurodegeneration in Parkinson's disease mouse model. *NPJ Parkinsons Dis.* **10**, 32 (2024).
31. Xia, Y. et al. Microglia as modulators of exosomal alpha-synuclein transmission. *Cell Death Dis.* **10**, 174 (2019).
32. Bosse, R. & Di Paolo, T. Dopamine and GABAA receptor imbalance after ovariectomy in rats: model of menopause. *J. Psychiatry Neurosci.* **20**, 364–371 (1995).
33. Bosse, R., Rivest, R. & Di Paolo, T. Ovariectomy and estradiol treatment affect the dopamine transporter and its gene expression in the rat brain. *Brain Res Mol. Brain Res.* **46**, 343–346 (1997).
34. Marshall, J. F. & Ungerstedt, U. Supersensitivity to apomorphine following destruction of the ascending dopamine neurons: quantification using the rotational model. *Eur. J. Pharm.* **41**, 361–367 (1977).
35. Hudson, J. L. et al. Correlation of apomorphine- and amphetamine-induced turning with nigrostriatal dopamine content in unilateral 6-hydroxydopamine lesioned rats. *Brain Res.* **626**, 167–174 (1993).
36. Matityahu, L. et al. Acetylcholine waves and dopamine release in the striatum. *Nat. Commun.* **14**, 6852 (2023).
37. Cordeau, P. Jr., Lalancette-Hébert, M., Weng, Y. C. & Kriz, J. Live imaging of neuroinflammation reveals sex and estrogen effects on astrocyte response to ischemic injury. *Stroke* **39**, 935–942 (2008).
38. Ishida, Y., Nagai, A., Kobayashi, S. & Kim, S. U. Upregulation of protease-activated receptor-1 in astrocytes in Parkinson disease: astrocyte-mediated neuroprotection through increased levels of glutathione peroxidase. *J. Neuropathol. Exp. Neurol.* **65**, 66–77 (2006).
39. Cheng, X. Y. et al. Human iPSCs derived astrocytes rescue rotenone-induced mitochondrial dysfunction and dopaminergic neurodegeneration in vitro by donating functional mitochondria. *Transl. Neurodegener.* **9**, 13 (2020).
40. Loria, F. et al. alpha-Synuclein transfer between neurons and astrocytes indicates that astrocytes play a role in degradation rather than in spreading. *Acta Neuropathol.* **134**, 789–808 (2017).
41. Bancroft, E. A., De La Mora, M., Pandey, G., Zarate, S. M. & Srinivasan, R. Extracellular S100B inhibits A-type voltage-gated potassium currents and increases L-type voltage-gated calcium channel activity in dopaminergic neurons. *Glia* **70**, 2330–2347 (2022).
42. Shytle, R. D. et al. Cholinergic modulation of microglial activation by alpha 7 nicotinic receptors. *J. Neurochem* **89**, 337–343 (2004).
43. Wu, S. Y. et al. Estrogen ameliorates microglial activation by inhibiting the Kir2.1 inward-rectifier K(+) channel. *Sci. Rep.* **6**, 22864 (2016).
44. Moen, J. K. & Lee, A. M. Sex Differences in the Nicotinic Acetylcholine Receptor System of Rodents: Impacts on Nicotine and Alcohol Reward Behaviors. *Front Neurosci.* **15**, 745783 (2021).
45. Paradiso, K., Zhang, J. & Steinbach, J. H. The C terminus of the human nicotinic alpha4beta2 receptor forms a binding site required for potentiation by an estrogenic steroid. *J. Neurosci.* **21**, 6561–6568 (2001).
46. Jin, X. & Steinbach, J. H. A portable site: a binding element for 17β-estradiol can be placed on any subunit of a nicotinic α4β2 receptor. *J. Neurosci.* **31**, 5045–5054 (2011).
47. Cummings, J. A., Jagannathan, L., Jackson, L. R. & Becker, J. B. Sex differences in the effects of estradiol in the nucleus accumbens and striatum on the response to cocaine: neurochemistry and behavior. *Drug Alcohol Depend.* **135**, 22–28 (2014).
48. Becker, J. B. Estrogen rapidly potentiates amphetamine-induced striatal dopamine release and rotational behavior during microdialysis. *Neurosci. Lett.* **118**, 169–171 (1990).

Acknowledgements

This study was funded by a National Institutes of Health (NIH) research grant, R01NS115809 to RS.

Author contributions

S.M.Z., R.C.G. and G.P. performed experiments, analyzed data, interpreted results and wrote the manuscript. R.S. conceptualized the study, designed experiments, supervised S.M.Z., R.C.G. and G.P., provided resources and funding for the study, and wrote and edited the manuscript.

Competing interests

The authors declare no competing interests.

Additional information

Correspondence and requests for materials should be addressed to Rahul Srinivasan.